RSC Advances

PAPER

View Article Online
View Journal | View Issue

Cite this: *RSC Adv.*, 2015, **5**, 31845

Influence of side-chain interactions on the self-assembly of discotic tricarboxyamides: a crystallographic insight†

Arpita Paikar, Apurba Pramanik and Debasish Haldar*

Received 4th March 2015
Accepted 27th March 2015

DOI: 10.1039/c5ra03864b

www.rsc.org/advances

Different assembly and behaviour of homologous discotic tricarboxyamides containing β-alanine and γ-aminobutyric acid have been investigated. From UV/Vis and FT-IR spectroscopy the tricarboxyamides have similar self-assembly patterns. But, the tricarboxyamide **2** containing γ-aminobutyric acid residues forms a gel in aromatic solvents after heating, cooling and ageing. However, the β-alanine analogue **1** failed to form a gel under the same conditions. From FE-SEM studies the tricarboxyamide **1** shows unbranched rod like morphology but the tricarboxyamide **2** exhibits an entangled fiber network. Finally, the X-ray crystallography reveals that both the tricarboxyamides **1** and **2** adopt 3-fold intermolecular H-bonded helical columnar structures. Detailed structural analysis shows that the individual helical columnar structures of tricarboxyamide **2** are themselves self-assembled through multiple hydrophobic interactions between side chains and thereby form a supramolecular network structure. However, the tricarboxyamide **1** columns are self-assembled into a supramolecular bundle-like structure. The result indicates that side chain interactions have a drastic effect on quaternary structure and function.

Introduction

Side-chain/side-chain interactions[1] within and between different secondary structures are key to the stabilization of the tertiary and quaternary structures of peptides and proteins.[2] The 20 natural amino acids differ by only side-chain structures.[3] Side-chain/side-chain interactions have a dominant role in folded protein structures.[4] But the role of side-chain interactions in the peptide mimetic is largely unexplored.[5–7] Hence, the design and synthesis of building blocks with side chains having tuneable functionality is highly important for this bottom-up approach.[8] Moreover, the building blocks need a delicate balance of the intramolecular and intermolecular non-covalent interactions.[9] Various building blocks with π-systems as core have been discussed in a recent review.[10] In this context, the use of 1,3,5-benzenetricarboxamide derivatives to direct the self-assembly has opened up a new window for material science.[11] Generally, 1,3,5-benzenetricarboxamide derivatives formed a columnar structure due to the co-operative three fold helical hydrogen bonds among the consecutive amide groups between neighbour molecules.[11] Versatile tricarboxyamide derivatives have been synthesized by incorporating diverse functional groups such as alkyl,[12] aryl,[13] pyridyl,[14] bipyridyl,[15] porphyrinyl,[16] triphenylyl,[17] oligo(*p*-phenylenevinylene),[18] amino acid,[19] dipeptide,[20] oligopeptide,[21] oligo-(ethyleneoxy),[22] and benzocrown ethers.[23] Meijer and co-workers have used 1,3,5-benzenetricarboxamide derivatives as MRI contrast reagents.[24] Matsunaga *et al.* have reported the development of liquid crystals from 1,3,5-benzenetricarboxamide.[25] Gelinsky *et al.* have used 1,3,5-benzenetricarboxamide derivatives as metal complexation agents.[26] Broaders *et al.* have developed a drug delivery vehicle exploiting 1,3,5-benzenetricarboxamide derivatives.[27] Recently, we have reported the fabrication of porous material from discotic tricarboxyamide containing tyrosine residues, through side chain–core interactions.[28]

Intrigued by the previous knowledge, we wanted to investigate the assembly of discotic tricarboxyamides with flexible hydrophobic side chains. Herein we present influence of side chain interactions on quaternary structure and function of tricarboxyamides. The tricarboxyamides **1** and **2** contain 1,3,5-benzene tricarboxylic acid and β-alanine and γ-aminobutyric acid. From UV/Vis, FT-IR and NMR spectroscopic studies the tricarboxyamides **1** and **2** have same self-assembly pattern. Interestingly the tricarboxyamide **2** containing γ-aminobutyric acid residues form organogel in aromatic solvents after heating, cooling and ageing. But the β-alanine analogue **1** failed to form gel under same condition. FE-SEM images show that the tricarboxyamide **1** has unbranched rod like morphology but the tricarboxyamide **2** has entangled fibers network. Single crystal X-ray diffraction studies exhibit that both the tricarboxyamide

Department of Chemical Sciences, Indian Institute of Science Education and Research Kolkata, Mohanpur, West Bengal 741246, India. E-mail: deba_h76@yahoo.com; deba_h76@iiserkol.ac.in; Fax: +91 3325873020; Tel: +91 3325873119

† Electronic supplementary information (ESI) available: Synthesis and characterization of trisamides, ^{1}H NMR, ^{13}C NMR, Fig. S1–S10. CCDC 1051708 and 1011367. For ESI and crystallographic data in CIF or other electronic format see DOI: 10.1039/c5ra03864b

1 and **2** adopts 3-fold intermolecular H-bonded helical columnar structure. In higher order, the tricarboxyamide **1** columns are self-assembled to form bundle-like structure. But, the individual helical columnar structure of tricarboxyamide **2** self-assembled through multiple hydrophobic interactions between side chains to form a supramolecular network structure.

Results and discussion

The discotic tricarboxyamides were designed with assumption that the rigid aromatic core leads to the threefold hydrogen bonded helical column and the achiral conformationally flexible β-alanine and γ-aminobutyric acids residues should adjust itself accordingly to help the process (Scheme 1). In this context the folding and interactions of hydrophobic groups will be interesting. Target tricarboxyamides **1** and **2** were synthesized by coupling benzene-1,3,5-tricarboxylic acid with β-alanine and γ-aminobutyric acids methyl ester. The synthesized compounds were purified and characterized by ^{1}H-NMR, ^{13}C-NMR, FT-IR and mass spectrometry (MS) analysis.

To investigate the self-assembly behaviour of tricarboxyamide **1** and **2**, a wide variety of different spectroscopic techniques have been used. The typical UV/Vis absorption spectra of tricarboxyamide **1** in methanol (0.023 mM) show an absorption band at 208 nm for π to π* transition (Fig. 1a). However, increasing the concentration of tricarboxyamide **1** induces stacking interactions between the molecules. The bathochromic shift of 17 nm of the absorption band with increasing concentration indicates J-type aggregation of tricarboxyamide **1**.[29] The absorption spectra of tricarboxyamide **2** in methanol also show an absorption band at 208 nm and bathochromic shift of 17 nm with increasing concentration (Fig. 1b). These results show that the tricarboxyamides **1** and **2** have similar aggregation pattern.

Solid state FT-IR spectroscopy is an excellent method to investigate the self-assembly propensity of the reported

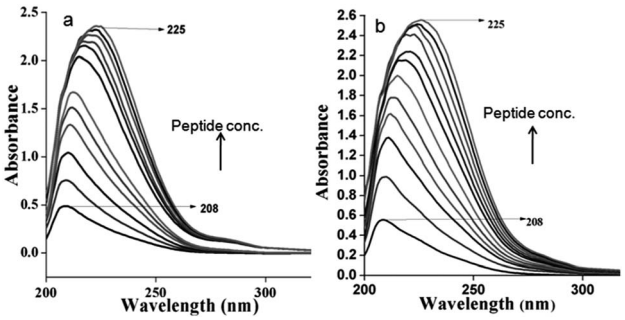

Fig. 1 Concentration dependent UV/Vis spectra of (a) tricarboxyamide **1** and (b) tricarboxyamide **2** showing J-type aggregation in methanol.

tricarboxyamides. In FT-IR, the region of 3500–3200 cm^{-1} is important for the N–H stretching vibrations however the range 1800–1500 cm^{-1} is assigned for the stretching band of amide I and the bending peak of amide II and ester groups. The FT-IR spectra of tricarboxyamide **1** (Fig. 2a) exhibits N–H stretching frequency at 3246 cm^{-1} for non hydrogen bonded N–H and amide peaks at 1637 and 1559 cm^{-1} indicating the presence of threefold intermolecular H-bonding between neighbouring molecules within the columnar structures.[30] The peak around 1741 cm^{-1} is responsible for the non hydrogen bonded ester carbonyls. The tricarboxyamide **2** exhibits peak at 3237 cm^{-1} for N–H stretching frequency. The amide and methyl ester have appeared at 1742, 1636 and 1562 cm^{-1} (Fig. 2b). These results indicate that the tricarboxyamides **1** and **2** have similar self-assembly propensity.

But, the tricarboxyamides exhibits different gelation behavior in aromatic solvents. The gelation propensities of tricarboxyamides **1** and **2** have been studied in a wide variety of organic solvents using conventional heating-cooling techniques.[31] However, the tricarboxyamides **1** did not form gel in aromatic hydrocarbon like toluene, *o*-xylene, *m*-xylene, *p*-xylene, 1,2-dichlorobenzene. But when solutions of the reported tricarboxyamides **2** in various organic solvents (ESI Table 1†) were

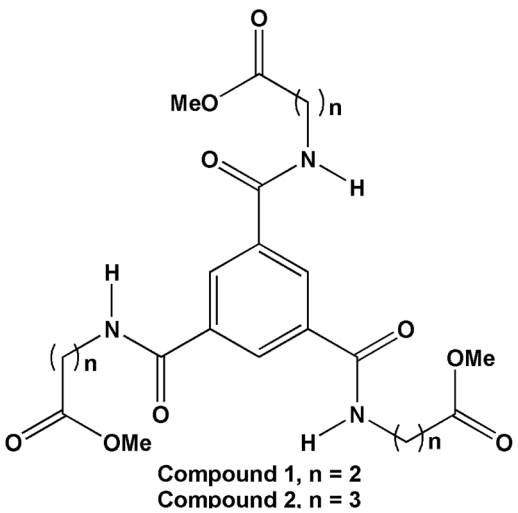

Scheme 1 The schematic presentation of tricarboxyamides **1** and **2**.

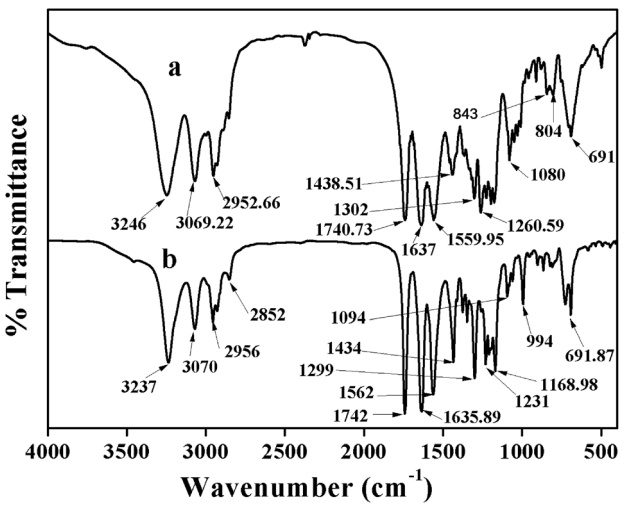

Fig. 2 Solid state FT-IR spectra of tricarboxyamides (a) **1** and (b) **2**.

subjected to heating-cooling techniques, homogeneous gelation in aromatic hydrocarbon like toluene, *o*-xylene, *m*-xylene, *p*-xylene was observed. The gelation has been confirmed by the inverted vial method.[32] The opaque gels of tricarboxyamides **2** are stable for 2–3 months at room temperature and the gels are thermoreversible (ESI†).

The information about the type of network (tertiary structure) responsible for the observed gelation of tricarboxyamide **2** in toluene was obtained from rheology. The storage modulus (G', a measure of the elastic response of the material) of the gel (10 wt%) was found to be larger than the loss modulus (G'', a measure of the viscous response), indicative of an elastic rather than viscous material (Fig. 3).[13] Such rheological behaviour is a characteristic of physically cross-linked gel *via* weak interactions.[13]

Further, to investigate the self-assembly behaviour of tricarboxyamide **2** in organogel, variable temperature ^{1}H NMR spectroscopic experiments have been performed. The experiments started with tricarboxyamide **2** gel in toluene-D_8. From the stack plot, the downfield shifts of amide protons upon heating suggest that the intermolecular three fold hydrogen bonds are broken with increasing temperature. Whereas the 1,3,5-benzene tricarboxylic acid protons exhibit upfield shifts up to 85 °C (gel melting temperature) and show downfield shifts at higher temperature (Fig. 4). Moreover, α, β and γ protons of γ-amino butyric acid residues exhibit significant downfield shifts upon heating which suggest that the intermolecular hydrophobic interactions are also changed with increasing temperature. The tricarboxyamide **1** does not form gel in toluene-D_8. Under same variable temperature ^{1}H NMR spectroscopic experiments, the tricarboxyamide **1** does not exhibit any significant shift of α and β protons of β-alanine residues (ESI Fig. S1†). Hence, not only the hydrogen bonding and π–π stacking interactions but also the hydrophobic interactions plays an important role in self-assembly and gelation of tricarboxyamide **2**.

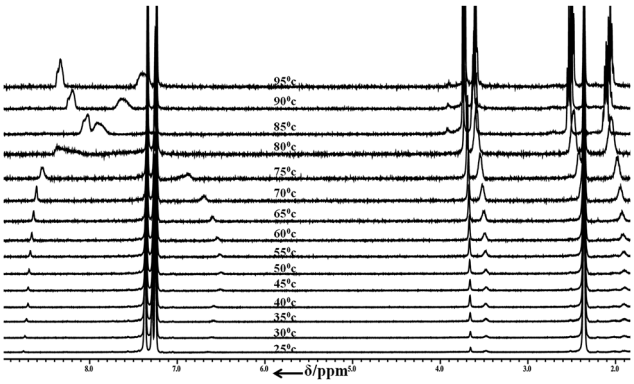

Fig. 4 Part of the ^{1}H NMR spectra of tricarboxyamide **2** gel in toluene-D_8 with increasing temperature.

The field emission scanning electron microscope (FE-SEM) has been used to study the morphology of the reported tricarboxyamide **2** xerogel obtained from various aromatic solvents. The FE-SEM micrographs of the corresponding xerogels from toluene, *o*-xylene, *m*-xylene and *p*-xylene exhibit the entangled networks of unbranched fibers with 1 μm average diameter and several micrometers in length (Fig. 5).

To examine the difference in morphology, we have also studied the solution of tricarboxyamides **1** or **2** in 1,2-dichloro benzene by field emission scanning electron microscope (FE-SEM). For FE-SEM, The freshly prepared solution of tricarboxyamides in 1,2-dichloro benzene (5 mg mL^{-1}) was drop-casted onto a silicon wafer and dried by slow evaporation. The material was then allowed to dry in a vacuum at 30 °C for two days. From FE-SEM image (Fig. 6a) the tricarboxyamide **1** exhibits unbranched polydisperse crystalline morphology. The crystals are very rigid and several micrometer in length. However, FE-SEM image of the tricarboxyamide **2** shows the entangled fibers network morphology (Fig. 6b). This three dimensional

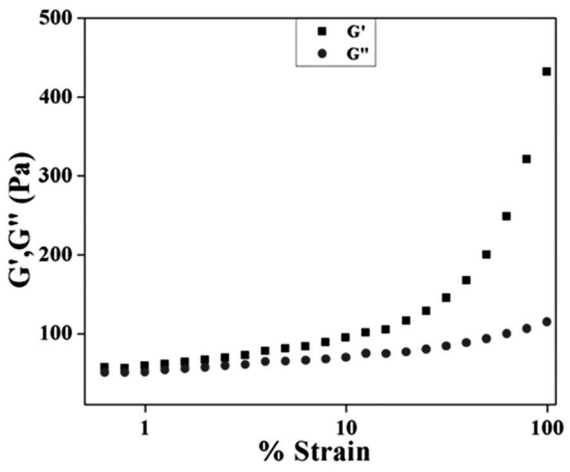

Fig. 3 Mechanical response of tricarboxyamide **2** gel in toluene at 20 °C with small oscillatory shear in the linear viscoelastic regime.

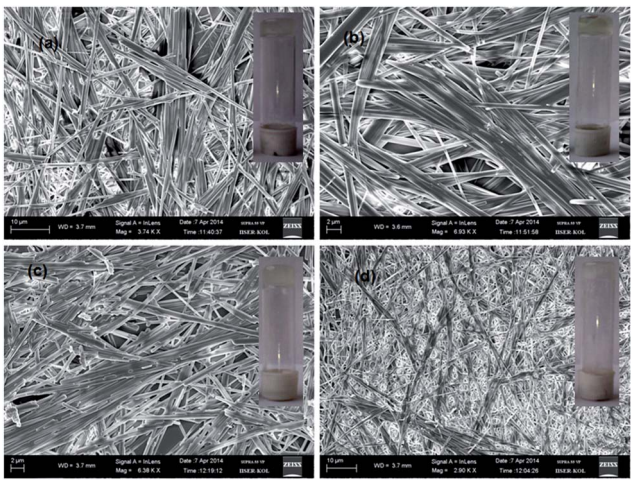

Fig. 5 FE-SEM images showing entangled networks of fibers of tricarboxyamide **2** xerogel from (a) toluene, (b) *o*-xylene, (c) *m*-xylene and (d) *p*-xylene. (Inset: the picture of the organogels).

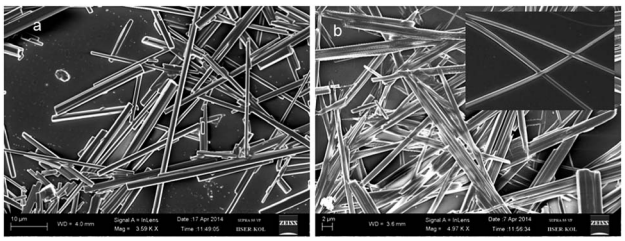

Fig. 6 (a) FE-SEM image of tricarboxyamide **1** showing unbranched polydisperse crystalline morphology. (b) FE-SEM image of tricarboxyamide **2** showing entangled fibers network. (Inset: multipoint entangled fibers).

network of entangled fibers (physical crosslinks) helps to entrap solvent molecules and forms organogel.[33]

Clear evidence of inter column interactions between side chains has confirmed by X-ray crystallography.[34] Tricarboxyamide **1** crystallizes with three molecules in the asymmetric unit (ESI Fig. S2†). The ORTEP diagram (ESI Fig. S2†) of tricarboxyamide **1** shows that the amide groups in a molecule are out of the central ring plane though two amides are tilted toward the same direction and third one in opposite direction. Two β-alanine residues adopt *gauche* conformation and third one adopts *anti* conformation (Fig. 7a). The torsion angles around the central benzene core and the β-alanine residues appears to play a critical role in dictating the overall structural features of tricarboxyamide **1**. Moreover, structure of **1** exhibit that the two β-alanine residues are in the same face and the third one is in the opposite face of the central benzene ring (Fig. 7a). From X-ray crystallography, it is evident that the asymmetric unit contains one molecule of tricarboxyamide **2**. The ORTEP diagram (ESI Fig. S3†) of tricarboxyamide **2** shows that two γ-aminoburytic acid residues adopt *gauche–gauche* conformation and third one adopts *gauche–anti* conformation (Fig. 7b). The amide groups are out of the central ring plane. However, aromatic amides prefer coplanarity of the carbonyl functional group with the aryl system to optimize conjugation, in tricarboxyamide **2** the amides are tilted toward the same direction (Fig. 7b). This is because of the competition between the demand of conjugation (amide and aryl) and that of intermolecular NH···O=C hydrogen bonding. The solid state structure of **2** exhibits that the two γ-amino butyric acids are in the same face and the third one is in the opposite face of the central benzene ring (Fig. 7b).

The crystal structure further reveals that the individual tricarboxyamide **1** subunits are stacked on top of another by threefold intermolecular H-bonding interaction between neighbouring molecules and generate a supramolecular column like structure (Fig. 8a) about crystallographic *c* direction.[35] The hydrogen bonding parameters of tricarboxyamides are listed in Table 1. The columnar arrangement also stabilized by strong π–π stacking interactions. The center-to-center distance between the benzene rings in columnar assembly is about 3.541 Å. The J-type aggregation of the tricarboxyamide **1** molecules helps to place the β-alanine residues in a regular helical manner outside of the columnar central aromatic core (Fig. 8a). Hence, the tricarboxyamide **1** column looks like a circular block on top view (Fig. 8b). The tricarboxyamide **2** also exhibits supramolecular columnar structure stabilized by 3-fold intermolecular H-bonding interactions in solid state.[35] The individual discotic tricarboxyamide **2** molecules are themselves stack one top of another and regularly interlinked through

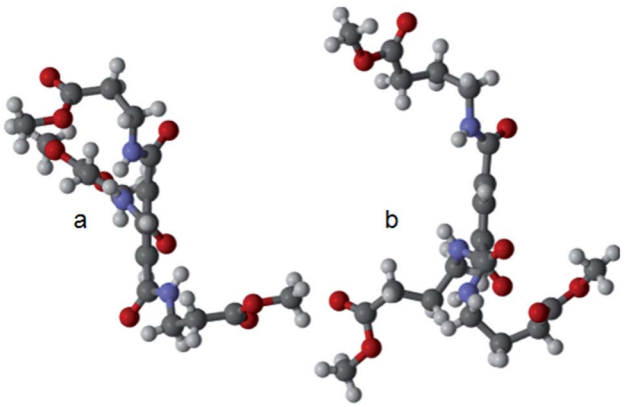

Fig. 7 The solid state structures of tricarboxyamides (a) **1** and (b) **2**.

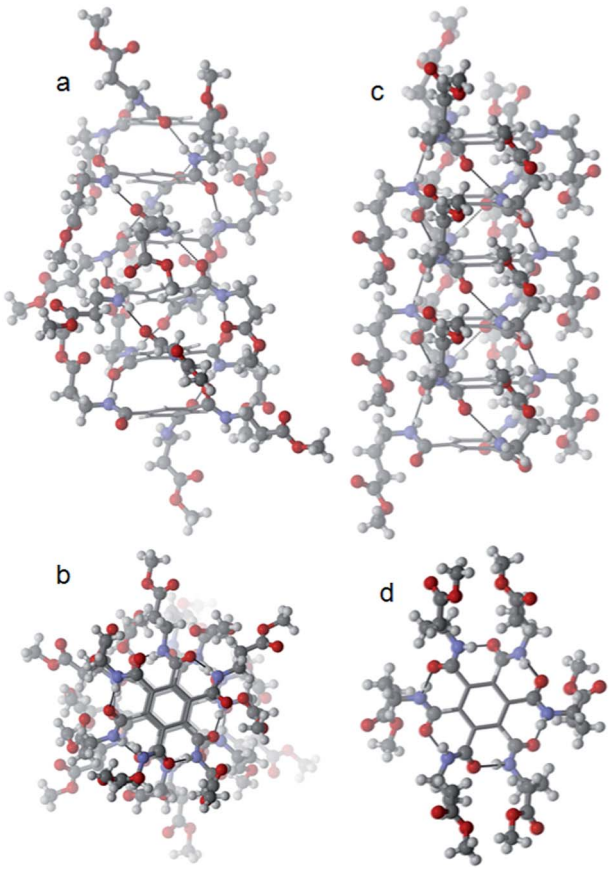

Fig. 8 (a) Side view and (b) top view packing presentation of the supramolecular column of tricarboxyamide **1**. (c) Side view and (d) top view of the supramolecular column of tricarboxyamide **2**. The intermolecular hydrogen bonds are presented as black dotted line.

Table 1 Hydrogen bonding parameters of tricarboxyamides **1** and **2**[a]

	D–H···A	D···H (Å)	H···A (Å)	D···A (Å)	D–H···A (°)
1	N1–H1···O12	0.86	2.08	2.920(6)	165
	N2–H2···O16	0.86	2.18	3.021(6)	167
	N3–H3···O13[a]	0.86	1.95	2.800(6)	168
	N4–H4···O3[b]	0.86	2.09	2.906(7)	158
	N5–H5···O7	0.86	1.96	2.796(6)	165
	N6–H6···O4[b]	0.86	2.09	2.945(7)	172
	N7–H7A···O21[c]	0.86	2.05	2.869(6)	159
	N8–H8···O22[d]	0.86	2.02	2.858(7)	166
	N9–H9···O25[c]	0.86	2.11	2.963(6)	171
2	N1–H1···O5[e]	0.86	2.04	2.861(3)	158
	N2–H2···O6[e]	0.86	2.06	2.873(3)	157
	N3–H3···O8[e]	0.86	2.02	2.856(3)	165

[a] Symmetry equivalent *a*: $1-x+y, 1-x, 1/3+z$, *b* = $1-y, x-y, -1/3+z$, *c* = $x-y, x, -1/6+z$, *d* = $y, -x+y, 1/6+z$, *e* = $1/2-x, -1/2+y, 1/2-z$.

intermolecular hydrogen bonding interactions (N1–H1···O5, N2–H2···O6, and N3–H3···O8) to form the helical columnar assembly along crystallographic *b* direction (Fig. 8c). There also exist a strong π–π interaction between adjacent aromatic ring. The centre-to-centre distance between the benzene rings in columnar assembly is about 3.486 Å. Outside of the columnar central aromatic core, the γ-amino butyric acid residues are hanging in linear fashion (Fig. 8c). Hence, the tricarboxyamide **2** column looks like a star on top view (Fig. 8d).

The packing diagram further reveals that the individual tricarboxyamide **1** columns are self-assembled and generate a supramolecular bundle-like framework along crystallographic *a* and *b* directions (Fig. 9). This type of packing leads to unbranched rod-like morphology for tricarboxyamide **1**. From X-ray crystallography, in higher order packing, the individual helical columnar structure of tricarboxyamide **2** are themselves self-assembled through multiple hydrophobic interactions (between γ-amino butyric acid's β methylenes and between ester methyl groups), and thereby form a supramolecular

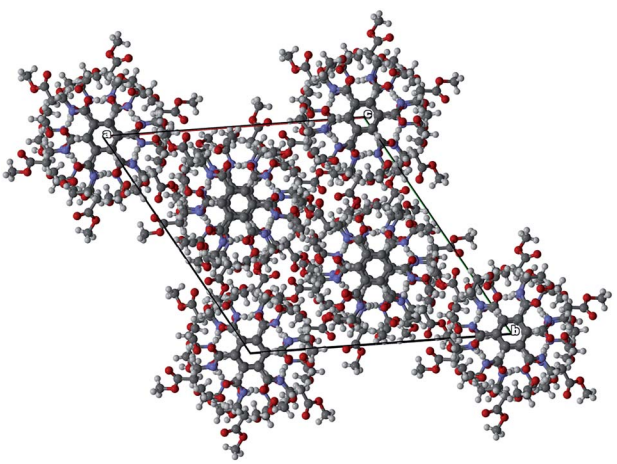

Fig. 9 The top view packing diagram of tricarboxyamide **1** showing honeycomb-like structure.

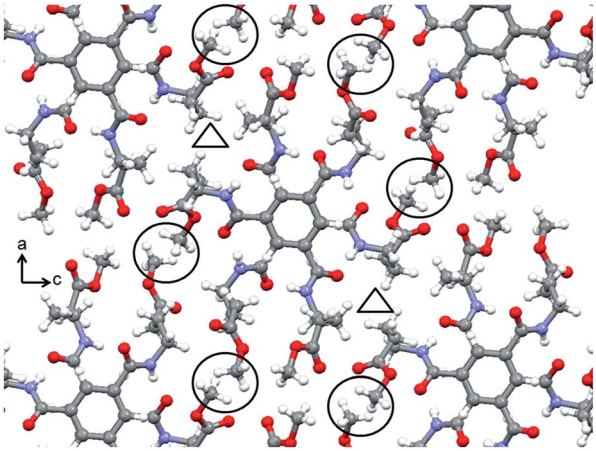

Fig. 10 Top view packing presentation of the supramolecular frameworks of tricarboxyamide **2** along crystallographic *a* and *b* directions. The circles and triangles are mark for hydrophobic interactions between side chains.

structure along the crystallographic *a* and *c* direction (Fig. 10). The intermolecular C–H···O hydrogen bonds[36] (C16–H16B···O7, 2.54 Å, 3.48 Å, 166°, $-1+x, y, z$) also help to stabilized the supramolecular structure. For tricarboxyamide **2**, the side-chains interactions (physical crosslinks) help to develop entangled fibers network morphology which entrap solvent molecules and forms organogel.

Conclusions

In conclusion, the self-assembly propensities of a series of discotic tricarboxyamides containing β-alanine and γ-aminobutyric acid has been reported. The tricarboxyamide with γ-aminobutyric acid residues form entangled fibers network and thermo responsive gel in aromatic solvents but the β-alanine analogue failed to form gel under same conditions. The X-ray crystallography reveals that the both the tricarboxyamide **1** and **2** adopts 3-fold intermolecular H-bonded helical columnar structure. The individual helical columnar structure of tricarboxyamide **2** is further self-assembled through multiple hydrophobic interactions between side chains and forms a supramolecular network structure. But the tricarboxyamide **1** columns are self-assembled to form bundle-like structure. The result presented here may foster new studies on side chain interactions for diverse applications.

Experimental

General

All amino acids were purchased from Sigma chemicals. HOBt (1-hydroxybenzotriazole) and DCC (dicyclohexylcarbodiimide) were purchased from SRL.

Tricarboxyamides synthesis

The tricarboxyamide were synthesized by conventional solution-phase methods. The C-terminus of amino acids was protected

as a methyl ester. The products were purified by column chromatography using silica (100–200 mesh size) gel as a stationary phase and an *n*-hexane–ethyl acetate mixture as an eluent. The intermediates and final compounds were fully characterized by 500 MHz and 400 MHz ^{1}H NMR spectroscopy, 100 MHz ^{13}C NMR spectroscopy, FT-IR spectroscopy and mass spectrometry. The tricarboxyamides **1** and **2** were also characterized by X-ray crystallography.

Tricarboxyamide (1). Dry triethylamine (NEt_3; 0.76 mL, 5.44 mmol) was added to an ice-cooled solution of β-Ala-OMe·HCl (0.345 g, 2.4705 mmol) in dry CH_2Cl_2 (20 mL) and the mixture was stirred for 20 min. Benzene-1,3,5-tricarbonyl trichloride (0.145 g, 0.549 mmol) dissolved in dry CH_2Cl_2 (25 mL) was added dropwise for 15 min and left to stir for 24 h under nitrogen atmosphere. After completion of reaction CH_2Cl_2 was evaporated under reduced pressure and the residue was dissolved in ethyl acetate (60 mL). The organic layer was washed with 2 M HCl (3 × 50 mL), brine (2 × 50 mL), 1 M sodium carbonate (3 × 50 mL) and brine (2 × 50 mL) and dried over anhydrous sodium sulfate. It was evaporated under a vacuum to yield tricarboxyamide **1** as a off-white solid. Chromatographic purification by 100–200 mesh using 1 : 2 (EtOAc : hexane) as eluent of the crude product yielded 0.326 g of **1**. Yield 31.46%.

^{1}H NMR (400 MHz, $CDCl_3$, δ in ppm): 8.331 (s, 3H, aromatic ring proton), 7.763–7.734 (t, 3H, J = 5.8 Hz, NH), 3.649–3.633 (d, 6H, J = 6.4 Hz, $C^{\beta}H$ of β-Ala), 3.614 (s, 9H, OCH_3), 2.624–2.593 (t, 6H, J = 6.2 Hz $C^{\alpha}H$ of β-Ala). ^{13}C NMR (100 MHz, $CDCl_3$, δ in ppm): 173.172, 166.793, 134.881, 129.246, 52.292, 36.360, 33.948. Mass spectra: m/z 488.1751, $[M + Na]^+$; M calcd 465.2.

Tricarboxyamide (2). Dry triethylamine (NEt_3; 0.76 mL, 5.44 mmol) was added to an ice-cooled solution of Gaba-OMe·HCl (0.379 g, 2.4705 mmol) in dry CH_2Cl_2 (20 mL) and the mixture was stirred for 20 min. Benzene-1,3,5-tricarbonyl trichloride (0.145 g, 0.549 mmol) dissolved in dry CH_2Cl_2 (25 mL) was added dropwise for 15 min and left to stir for 24 h under nitrogen. After completion of reaction CH_2Cl_2 was evaporated under reduced pressure and the residue was dissolved in ethyl acetate (60 mL). The organic layer was washed with 2 M HCl (3 × 50 mL), brine (2 × 50 mL), 1 M sodium carbonate (3 × 50 mL) and brine (2 × 50 mL) and dried over anhydrous sodium sulfate. It was evaporated in a vacuum to yield tricarboxyamide **2** as a off-white solid. Chromatographic purification by 100–200 mesh using 1 : 2 (EtOAc : hexane) as eluent of the crude product yielded 0.4166 g of **2**. Yield 33.27%.

^{1}H NMR (500 MHz, $CDCl_3$, δ in ppm): 8.007 (s, 3H, aromatic ring proton), 7.842–7.821 (t, 3H, J = 5.25 Hz, NH), 3.561 (s, 9H, OCH_3), 3.330–3.292 (q, 6H, J = 6.33 Hz, $C^{\gamma}H$ of Gaba), 2.317–2.288 (t, 6H, J = 7.25 Hz $C^{\alpha}H$ of Gaba), 1.808–1.1780 (t, 6H, J = 7 Hz $C^{\beta}H$ of Gaba). ^{13}C NMR (100 MHz, $CDCl_3$, δ in ppm): 173.595, 166.697, 134.920, 128.097, 51.481, 39.357, 31.175, 24.257. Mass spectra: m/z 530.1033, $[M + Na]^+$; M calcd 507.2.

NMR experiments

All NMR studies were carried out on a Brüker AVANCE 500 MHz spectrometer at 278 K. Compound concentrations were in the range 1–10 mM in $CDCl_3$.

FT-IR spectroscopy

All reported solid-state FT-IR spectra were obtained with a Perkin Elmer Spectrum RX1 spectrophotometer with the KBr disk technique.

UV/Vis spectroscopy

UV/Vis absorption spectra were recorded on a UV/Vis spectrophotometer (Hitachi).

Mass spectrometry

Mass spectra were recorded on a Q-Tof Micro YA263 high-resolution (Waters Corporation) mass spectrometer by positive-mode electrospray ionization.

Field emission scanning electron microscopy

Morphologies of all reported compounds were investigated using field emission-scanning electron microscopy (FE-SEM). A small amount of gel/solution of the corresponding compound was placed on a clean silicon wafer and then dried by slow evaporation. The material was then allowed to dry under vacuum at 30 °C for two days. The materials were gold-coated, and the micrographs were taken in an FE-SEM apparatus (Jeol Scanning Microscope-JSM-6700F).

Single crystal X-ray diffraction study

Intensity data of tricarboxyamides **1** and **2** crystals were collected with MoKα radiation using Bruker APEX-2 CCD diffractometer. Data were processed using the Bruker SAINT package and the structure solution and refinement procedures were performed using SHELX97.†[37]

Acknowledgements

We acknowledge the CSIR, India, for financial assistance (Project no. 01/2507/11-EMR-II). A. Paikar acknowledges the UGC, India for research fellowship. A. Pramanik thanks CSIR, India for fellowship.

Notes and references

1 M. M. Cox and D. L. Nelson, *Principles of Biochemistry*, W. H. Freeman and Company, New York, 5th edn, 2008.

2 (*a*) K. Berka, R. Laskowski, K. E. Riley, P. Hobza and J. Vondrášek, *J. Chem. Theory Comput.*, 2009, **5**, 982–992; (*b*) C. Zehe, M. Schmidt, R. Siegel, K. Kreger, V. Daebel, S. Ganzleben, H. W. Schmidt and J. Senker, *CrystEngComm*, 2014, **16**, 9273–9283; (*c*) A. Thomas, R. Meurisse, B. Charloteaux and R. Brasseur, *Proteins*, 2002, **48**, 628–634; (*d*) J. Gsponer, U. Haberthür and A. Caflisch, *Proc. Natl. Acad. Sci. U. S. A.*, 2003, **100**, 5154–5159.

3 V. Z. Spassov, L. Yan and P. K. Flook, *Protein Sci.*, 2007, **16**, 494–506.

4 (*a*) A. F. Pereira de Araujo, T. C. Pochapsky and B. Joughin, *Biophys. J.*, 1999, **76**, 2319–2328; (*b*) K. Berka,

R. A. Laskowski, P. Hobza and J. Vondrášek, *J. Chem. Theory Comput.*, 2010, **6**, 2191–2203.
5 S. V. Jadhav, A. Bandyopadhyaya and H. N. Gopi, *Org. Biomol. Chem.*, 2013, **11**, 509–514.
6 V. Azzarito, K. Long, N. S. Murphy and A. J. Wilson, *Nat. Chem.*, 2013, **5**, 161–173.
7 W. A. Loughlin, J. D. A. Tyndall, M. P. Glenn and D. P. Fairlie, *Chem. Rev.*, 2004, **104**, 6085–6118.
8 (*a*) D. Haldar, H. Jiang, J. M. Léger and I. Huc, *Angew. Chem., Int. Ed.*, 2006, **45**, 5483–5486; (*b*) J. Yan, W. Li and A. Zhang, *Chem. Commun.*, 2014, **50**, 12221–12233.
9 (*a*) D. J. Hill, M. J. Mio, R. B. Prince, T. S. Hughes and J. S. Moore, *Chem. Rev.*, 2001, **101**, 3893–4012; (*b*) L. G. Milroy, T. N. Grossmann, S. Hennig, L. Brunsveld and C. Ottmann, *Chem. Rev.*, 2014, **114**, 4695–4748; (*c*) J. Pal, S. Sanwaria, R. Srivastava, B. Nandan, A. Horechyy, M. Stammb and H. L. Chen, *J. Mater. Chem.*, 2012, **22**, 25102–25107.
10 S. S. Babu, V. K. Praveen and A. Ajayaghosh, *Chem. Rev.*, 2014, **114**, 1973–2129.
11 (*a*) S. Cantekin, T. F. A. de Greefab and A. R. A. Palmans, *Chem. Soc. Rev.*, 2012, **41**, 6125–6137; (*b*) Y. Ishioka, N. Minakuchi, M. Mizuhata and T. Maruyama, *Soft Matter*, 2014, **10**, 965–971.
12 P. J. M. Stals, J. C. Everts, R. de Bruijn, I. A. W. Filot, M. M. J. Smulders, R. Martín-Rapún, E. A. Pidko, T. F. A. de Greef, A. R. A. Palmans and E. W. Meijer, *Chem.–Eur. J.*, 2010, **16**, 810–821.
13 A. Bernet, R. Q. Albuquerque, M. Behr, S. T. Hoffmann and H.-W. Schmidt, *Soft Matter*, 2012, **8**, 66–69.
14 A. R. A. Palmans, J. A. J. M. Vekemans, E. W. Meijer, H. Kooijmans and A. L. Spek, *Chem. Commun.*, 1997, 2247–2248.
15 L. Brunsveld, H. Zhang, M. Glasbeek, J. A. J. M. Vekemans and E. W. Meijer, *J. Am. Chem. Soc.*, 2000, **122**, 6175–6182.
16 R. van Hameren, P. Schö, A. M. van Buul, J. Hoogboom, S. V. Lazarenko, J. W. Gerritsen, H. Engelkamp, P. C. M. Christianen, H. A. Heus, J. C. Maan, T. Rasing, S. Speller, A. E. Rowan, J. A. A. W. Elemans and R. J. M. Nolte, *Science*, 2006, **314**, 1430–1433.
17 I. Paraschiv, M. Giesbers, B. van Lagen, F. C. Grozema, R. D. Abellon, L. D. A. Siebbeles, A. T. M. Marcelis, H. Zuilhof and E. J. R. Sudhölter, *Chem. Mater.*, 2006, **18**, 968–974.
18 J. van Herrikhuyzen, P. Jonkheijm, A. P. H. J. Schenning and E. W. Meijer, *Org. Biomol. Chem.*, 2006, **4**, 1539–1545.
19 P. P. Bose, M. G. B. Drew, A. K. Das and A. Banerjee, *Chem. Commun.*, 2006, 3196–3198.
20 K. P. van den Hout, R. Martín-Rapún, J. A. J. M. Vekemans and E. W. Meijer, *Chem.–Eur. J.*, 2007, **13**, 8111–8123.
21 K. Matsuura, K. Murasato and N. Kimisuka, *J. Am. Chem. Soc.*, 2005, **127**, 10148–10149.
22 P. J. M. Stals, J. F. Haveman, R. Martín-Rapún, C. F. C. Fitié, A. R. A. Palmans and E. W. Meijer, *J. Mater. Chem.*, 2009, **19**, 124–130.
23 S. Lee, J.-S. Lee, C. H. Lee, Y.-S. Jung and J.-M. Kim, *Langmuir*, 2011, **27**, 1560–1564.
24 P. Besenius, J. L. M. Heynens, R. Straathof, M. M. L. Nieuwenhuizen, P. H. H. Bomans, E. Terreno, S. Aime, G. J. Strijkers, K. Nicolay and E. W. Meijer, *Contrast Media Mol. Imaging*, 2012, **7**, 356–361.
25 Y. Matsunaga, N. Miyajima, Y. Nakayasu, S. Sakai and M. Yonenaga, *Bull. Chem. Soc. Jpn.*, 1988, **61**, 207–210.
26 M. Gelinsky, R. Vogler and H. Vahrenkamp, *Inorg. Chem.*, 2002, **41**, 2560–2564.
27 K. E. Broaders, S. J. Pastine, S. Grandhe and J. M. J. Fréchet, *Chem. Commun.*, 2011, **47**, 665–667.
28 P. Jana, A. Paikar, S. Bera, S. K. Maity and D. Haldar, *Org. Lett.*, 2014, **16**, 38–41.
29 H. Wu, L. Xue, Y. Shi, Y. Chen and X. Li, *Langmuir*, 2011, **27**, 3074–3082.
30 T. F. A. de Greef, M. M. L. Nieuwenhuizen, P. J. M. Stals, C. F. C. Fitié, A. R. A. Palmans, R. P. Sijbesma and E. W. Meijer, *Chem. Commun.*, 2008, 4306–4308.
31 K. J. C. van Bommel, C. van der Pol, I. Muizebelt, A. Friggeri, A. Heeres, A. Meetsma, B. L. Feringa and J. van Esch, *Angew. Chem., Int. Ed.*, 2004, **43**, 1663–1667.
32 S. Maity, P. Jana and D. Haldar, *CrystEngComm*, 2011, **13**, 3064–3071.
33 (*a*) S. J. George, A. Ajayaghosh, P. Jonkheijm, A. P. H. J. Schenning and E. W. Meijer, *Angew. Chem., Int. Ed.*, 2004, **43**, 3422–3425; (*b*) S. E. Paramonov, H. W. Jun and J. D. Hartgerink, *J. Am. Chem. Soc.*, 2006, **128**, 7291–7298.
34 ESI.†
35 V. Nagarajan and V. R. Pedireddi, *Cryst. Growth Des.*, 2014, **14**, 1895–1901.
36 G. R. Desiraju and T. Steiner, *The Weak Hydrogen Bond*, Oxford Science Publication, 1999.
37 G. M. Sheldrick, *SHELX 97*, University of Göttingen, Germany, 1997.